Environmental Science & Technology

pubs.acs.org/est

Article

Periphyton Phosphorus Uptake in Response to Dynamic Concentrations in Streams: Assimilation and Changes to Intracellular Speciation

Nolan J. T. Pearce,* Chris T. Parsons, Sarah M. Pomfret, and Adam G. Yates

Cite This: *Environ. Sci. Technol.* 2023, 57, 4643−4655

Read Online

ACCESS | Metrics & More | Article Recommendations | Supporting Information

ABSTRACT: Effective modeling and management of phosphorus (P) losses from landscapes to receiving waterbodies requires an adequate understanding of P retention and remobilization along the terrestrial−aquatic continuum. Within aquatic ecosystems, the stream periphyton can transiently store bioavailable P through uptake and incorporation into biomass during subscouring and baseflow conditions. However, the capacity of stream periphyton to respond to dynamic P concentrations, which are ubiquitous in streams, is largely unknown. Our study used artificial streams to impose short periods (48 h) of high SRP concentration on stream periphyton acclimated to P scarcity. We examined periphyton P content and speciation through nuclear magnetic resonance spectroscopy to elucidate the intracellular storage and transformation of P taken up across a gradient of transiently elevated SRP availabilities. Our study demonstrates that the stream periphyton not only takes up significant quantities of P following a 48-h high P pulse but also sustains supplemental growth over extended periods of time (10 days), following the reestablishment of P scarcity by efficiently assimilating P stored as polyphosphates into functional biomass (i.e., phospho-monoesters and phospho-diesters). Although P uptake and intracellular storage approached an upper limit across the experimentally imposed SRP pulse gradient, our findings demonstrate the previously underappreciated extent to which the periphyton can modulate the timing and magnitude of P delivery from streams. Further elucidating these intricacies in the transient storage potential of periphyton highlights opportunities to enhance the predictive capacity of watershed nutrient models and potentially improve watershed P management.

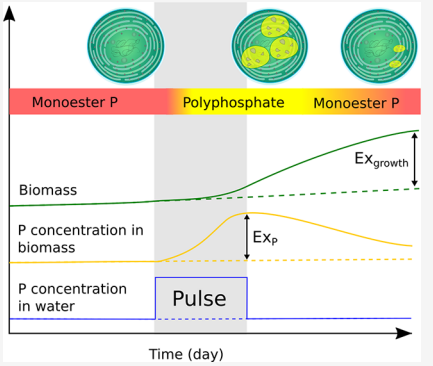

KEYWORDS: *phosphorus, periphyton, polyphosphate, pulse, P NMR*

1. INTRODUCTION

The biogeochemical flow of phosphorus (P) from the continents to the oceans is one of the most important processes regulating the stability and resilience of the Earth system.[1] However, the flux of P from land to receiving waterbodies has been dramatically altered during the last century. Globally, the application of P fertilizer has increased by an order of magnitude due to human and livestock population growth and a commensurate intensification of agricultural production.[2,3] The resulting augmentation, and changing speciation, of riverine P loads[4−6] from agricultural intensification has contributed to widespread eutrophication of freshwaters and coastal zones.[7,8] This has led to a concerted multidecadal effort by scientists, landowners, and policy makers to improve our understanding of P flows along the land to ocean continuum and limit P export to aquatic ecosystems.[7]

A considerable proportion of P exported from the landscape is retained within streams and rivers. However, the quantity retained is highly variable, both among watercourses and over time.[9−12] A variety of different physical and biogeochemical P-retaining mechanisms have been identified, which contribute to retention of total P (TP) within river channels.[12−18] Collectively, these P retaining mechanisms result in a spatially distributed set of legacy P pools within watersheds.[19,20] Many of the resultant storage mechanisms for legacy P pools are transient thereby acting to buffer surface water P concentrations, loads, and speciation on time scales ranging from minutes to decades.[11,16,21−24] Instream P storage, with its inherent temporal variability obfuscates the link between P export from the land, downstream delivery, and impacts to receiving water bodies, thereby rendering the whole watershed nutrient management effort a considerable challenge.[11,19,25] The current lack of a quantitative, mechanistic understanding of many P-buffering mechanisms along the terrestrial to aquatic continuum results in two key issues that limit the utility

Received: August 29, 2022
Revised: February 15, 2023
Accepted: February 15, 2023
Published: March 10, 2023

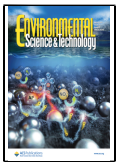

ACS Publications

© 2023 The Authors. Published by American Chemical Society

of watershed scale nutrient models as prognostic and diagnostic tools to assist policy makers in P-management decisions.

First, although assessment of long-term legacy P accumulation and depletion using a mass balance approach has been demonstrated in a number of watersheds (e.g., refs 26−28) few models are able to determine the spatial distribution of legacy-P within a watershed on time scales that can capture the dynamics of transient-P pools influencing the seasonal timing of P delivery to receiving water bodies. Second, due to an incomplete understanding of the chemical and physical characteristics of transient-P stores in watercourses, we have limited capacity to evaluate the risk, and timing, of P remobilization in response to changing hydrological, geochemical, or climatic drivers. Therefore, to manage P more effectively and mitigate eutrophication issues, we require a more nuanced understanding of the processes influencing P retention and remobilization along the terrestrial-aquatic continuum.[24,29]

Among the processes recognized to regulate P loads and concentrations in streams and rivers, assimilation by benthic periphyton and resultant excessive growth under low and subscouring flow conditions, has been identified as a pathway of global relevance.[30,31] However, the capacity of periphyton to respond to temporally dynamic P concentrations in streams, accumulate excess P under these conditions, and use that P to sustain growth over time is still incompletely understood. This is particularly true for mesotrophic and eutrophic streams, such as those covering large areas of the watersheds of the Lower Laurentian Great Lakes where the timing of P load delivery exerts an important control on the recurrence of nuisance and harmful algal blooms.[32]

Recent work has highlighted the potential of benthic periphyton to accumulate excess P in oligotrophic streams in response to short duration pulses of elevated P concentration.[33] Accumulation of excess P under conditions of high availability (i.e., luxury uptake) has also been observed in marine and freshwater phytoplankton[34−39] in addition to benthic algae.[40−42] Luxury uptake is achieved through intracellular conversion and storage of inorganic P molecules as polyphosphate polymers.[43] Polyphosphate accumulation may therefore serve as an underappreciated mechanism of transient P retention in streams that receive short duration high concentrations inputs of P from overland flows or episodic point sources. Despite this potential, there remains considerable uncertainty in the factors that regulate polyphosphate accumulation in periphyton and in the subsequent use of polyphosphate for the production of functional benthic periphyton biomass.

The goal of our study was to experimentally evaluate the response of benthic periphyton communities to dynamic P concentrations by using artificial streams to simulate P loading common to subscouring flow events occurring in natural streams draining agricultural catchments. A secondary goal was to identify the capacity of periphyton to store and subsequently use P accumulated in excess of immediate requirements. Specifically, our objectives were to (1) describe how periphyton P uptake and assimilation respond to a range of P concentrations delivered in short duration (48-h) pulses and (2) evaluate how intracellular P speciation of benthic periphyton changes with the assimilation and subsequent use of P acquired during short duration, high P concentration events.

2. MATERIALS AND METHODS

2.1. Experimental Design. A 26-day P addition experiment was conducted in nine artificial streams (see section 2.2). Initially, each stream received flowing surface water with a P concentration of 10 μg L^{-1} soluble reactive phosphorus (SRP) to allow periphyton to acclimate and establish under identical conditions. After a period of 13 days, each stream received a 48-h pulse of surface water with an individual higher SRP concentration (25, 50, 100, 150, 200, 250, 300, 400, or 700 ug L^{-1} SRP) creating an experimental SRP pulse treatment gradient. SRP concentrations were subsequently returned to 10 μg L^{-1} SRP for the remaining 11 days of the experiment. The potential for N limitation was minimized by maintaining total nitrogen at a constant concentration of 1500 μg N L^{-1}, in excess of established limitation concentrations.[44,45] Experimental SRP concentrations and the duration of elevated SRP concentrations were based on event-flow monitoring data collected from southern Ontario rivers draining agriculturally dominated watersheds free from point source P contributions where 10 μg L^{-1} SRP represented apparent background concentrations and concentrations of 25 to 700 μg L^{-1} SRP were observed during flow events.[46−49]

2.2. Artificial Streams. Our experiment was conducted outdoors at the Thames River Experimental Stream Sciences (TRESS) Center in London, Ontario, Canada from July 26 to August 21, 2018. Artificial streams (N = 9) used to conduct our experiment consisted of partially recirculating sinuous flumes (0.15 m deep by 0.20 m wide by 7.0 m long) with a 150 L reservoir (2.5 h water residence time) that received a continuous supply of low nutrient (TN = 406 μg L^{-1}; TP < 1 μg L^{-1}) carbon filtered water from the Lake Huron Water Supply System delivered through individual diaphragm pumps (pH = 7.93 to 8.08; alkalinity = 73 to 92 mg L^{-1} $CaCO_3$). Concentrated SRP (KH_2PO_4) was added to the water through individual dosing pumps connected to the outflow of each diaphragm pump and concentrated nitrogen (NH_4NO_3) was added with a single dosing pump to the common water supply of the facility. Flow rates of dosing and diaphragm pumps were calibrated daily to maintain desired nutrient concentrations. Water and nutrients delivered to each artificial stream were circulated with a flow-controlled, impeller pump. Discharge, light availability, daily water temperature, and substrate were controlled among all artificial streams at 150 cm^3/s, 60% shade (63.3 ± 17.6 mol m^{-2} day^{-1}), 21.5 °C (±1.0 °C), and cobble (D_{50} = 46 mm), respectively.

Periphyton from multiple natural streams were used to inoculate the artificial streams with biota adapted to regional conditions following Pearce et al.[15] (Table S1). Most of the inoculum was obtained by relocating quarried river rock that were anchored in plastic mesh bags (2 × 2 cm) in a nearby stream (Medway Creek) for about 4 weeks before the experiment. However, to increase community diversity, additional periphyton inoculum were collected by removing biofilm from randomly selected cobble substrates (5 to 10 cobbles) from five regional streams that varied in ambient P concentration (19.6 μg L^{-1} TP to 229.5 μg L^{-1} TP). All streams were indicative of P limitation with molar N:P ratios ranging from 36 to 388.

Collected biofilms from each of the five locations were mixed/blended into a slurry and distributed evenly among artificial streams. Based on past experiments with the same starting conditions (i.e., 10 μg L^{-1} SRP) as this experiment, the

https://doi.org/10.1021/acs.est.2c06285
Environ. Sci. Technol. 2023, 57, 4643−4655

inoculum results in an algal assemblage that is approximately 65% Bacilliariophyta and 30% Chloropyhta.[15] Charophyta and Cyanobacteria make up the remaining fractions.[15]

Unglazed ceramic tiles (4.7 × 4.7 cm) were used as an artificial substratum for periphyton. Tiles were placed on top of the precolonized cobble substrate at the start of the experiment immediately prior to the blended inoculum being added. Care was taken to only use very coarse cobble substrate as to limit the surface area available for abiotic sorption processes.

2.3. Sample Collection and Analysis. Periphyton was sampled 1 day before, 1 day after, and 10 days after experimental SRP pulses for periphyton P concentration and biomass (i.e., chlorophyll *a* and ash-free dry-mass). Samples collected for periphyton P speciation were restricted to just those collected after the SRP pulses to provide sufficient biomass for laboratory analyses. A composite and replicate sampling approach was implemented to account for spatial variability in periphyton communities within artificial streams. Periphyton were collected in composite samples for each analytical measurement by scraping a defined area of biofilm from randomly selected unglazed ceramic tiles. Three replicate samples were collected for periphyton P concentration, chlorophyll *a* and ash-free dry-mass whereby each replicate contained a composite of biofilm sampled from two separate tiles (10.62 cm^2). One sample was collected for P speciation analysis with P NMR and contained approximately 15 mL of wet biofilm sampled from five separate tiles.

Samples collected for periphyton P concentration were analyzed following the total P method of Aspila et al.,[50] and reported as mass per periphyton dry weight. Briefly, samples were freeze-dried for 48 h, ashed at 550 °C for 2 h, dissolved in 1.0 N HCl for 16 h then filtered to 0.45 μm. The resultant solution was analyzed by ICP-OES after appropriate dilution. Matrix-matched standards were used for all calibrations and NIST validated solutions were used as controls. Analysis of spiked samples consistently resulted in total P recoveries within 10% of expected values and certified reference materials analyzed during the same runs were within the certification range.

Periphyton P concentration was used to estimate P net uptake rate (U; μg-P m^{-2} s^{-1}) based on the surface area standardized difference in periphyton P concentration between samples collected 1 day before and 1 day after the SRP pulse, as well as between samples collected 1 day after and 10 days after the SRP pulse. Therefore, the P uptake rate presented herein represents the apparent uptake rate integrated over 48 and 240 h, respectively.

Samples collected for periphyton P speciation analysis were flash frozen in liquid nitrogen, stored at −80 °C then freeze-dried for 48 h prior to analysis. Freeze-dried biomass samples were extracted for solution ^{31}P NMR analysis following the protocol detailed by Cade-Menun.[51] This method has been shown to be capable of detecting and quantifying a broad variety of organic P forms in diverse environmental samples including phosphonates, orthophosphate monoesters, orthophosphate diesters, and polyphosphates.[51−56] Briefly, 0.2 g of dry biomass was mixed with 25 mL of extraction solution (0.25 M NaOH and 0.05 M Na_2EDTA) and shaken at ∼21 °C for 4 h. The mixture was then centrifuged at 2300 *g* for 20 min, the supernatant extracted by pipet, neutralized to pH 7 through the addition of ∼2.5 mL of 3 M HCl to avoid the degradation of polyphosphates and filtered to 0.45 μm (Nylon membrane).[57] A 1 mL aliquot of the filtrate was collected for analysis of Al, Ca, Fe, Mg, Mn, and P concentration by ICP-OES to assess P recovery from dry biomass and concentrations of paramagnetic ions (Fe and Mn) which influence NMR experiments. The NaOH−Na_2EDTA method resulted in near complete P extraction from biomass samples with extraction efficiency approximately equal to that achieved using the total P method detailed above (± 10%).[50] The remainder of the filtrate was frozen at −80 °C and freeze-dried for 48 h. Prior to NMR analysis, the dry material was redissolved in 0.650 mL of D_2O, 0.325 mL of 10 M NaOH, and 0.325 mL of extraction solution for 10 min, assisted by occasional vortexing, then centrifuged at 2300 g for 20 min. Subsequently, 1 mL of this solution, with an estimated pH > 12 was transferred to a 5 mm NMR tube for immediate analysis.[51]

Solution ^{31}P NMR spectra were acquired on a Bruker Avance 500 MHz (11.74 T) Ultrashield NMR spectrometer, equipped with a Quattro Nucleus Probe, operating at 202.45 MHz for ^{31}P, at the University of Waterloo NMR facility. Acquisition parameters were 90° pulse, 0.73 s acquisition time, and 10 s pulse delay, using a power-gated decoupling sequence at 25 °C. The acquisition parameters are similar to those used by many other ^{31}P NMR studies on environmental samples (e.g., refs 51, 58, 59) and were chosen to achieve acceptable spectra for the samples with the lowest P concentrations while avoiding overly long NMR experiments which can result in sample degradation due to hydrolysis at high pH.[59] The pulse delay time was set to 10 s to allow for near complete spin−lattice relaxation for all species (at least 4 to 5× estimated T_1) to avoid saturation and ensure accurate quantification of each compound class. T_1 times were estimated at between 0.8 and 2.5 s based on P:(Fe+Mn) (w/v) ratios in NaOH-Na_2EDTA extracts of 1.7 and 7.6, using the relationship described in McDowell et al.[60] A total of 4096 scans were collected per sample resulting in 12-h NMR experiments. Spectra were processed with 10 Hz line broadening then phase and baseline corrected using Bruker TopSpin 3.6.1 software. Relatively good peak separation was achieved (Figures S1−S3), likely in part due to relatively high P:(Fe+Mn) w/v ratios in biomass samples resulting in slow relaxation times.[60] Resultant peaks were integrated using Fityk 1.2.1 software.[61] P compound classes were identified by their chemical shifts relative to an external 85% orthophosphoric acid standard.[51,62] Shifts of −17.4 to −21.7 were classified as polyphosphate mid chain groups (i.e., present in phosphorus storage molecules), −8.8 to −10.5 as adenosine triphosphate (ATP) or similar molecules involved in the electron transport train (e.g., ADP, NAD, NADPH), −4.5 to −4.3 as pyrophosphate, −4.2 to −3.4 as polyphosphate end groups, −1.8 to 1.15 as phosphate diesters (e.g., DNA and phospholipids), 3.5 to 5.2 as phosphate monoesters (e.g., phosphate sugars), and 6 as orthophosphate (i.e., free phosphate in solution as well as contributions from other phosphate containing compounds) (Figures S1 and S3).

The concentration of each P compound class was determined by multiplying the combined fractional area of all peaks within the corresponding chemical shift range for that P compound class (e.g., 3.5 to 5.2 for phosphate monoesters, corresponding to the integration of the red line in Figure S3A) by the total P concentration for that sample. Compound class assignments were verified by spiking replicate algal samples with glucose 6 phosphate (G6P) and adenosine 5 triphosphate (ATP) and comparing the resultant chemical shift to those reported in the peak library provided by Cade-Menun.[51] Care

https://doi.org/10.1021/acs.est.2c06285
Environ. Sci. Technol. 2023, 57, 4643−4655

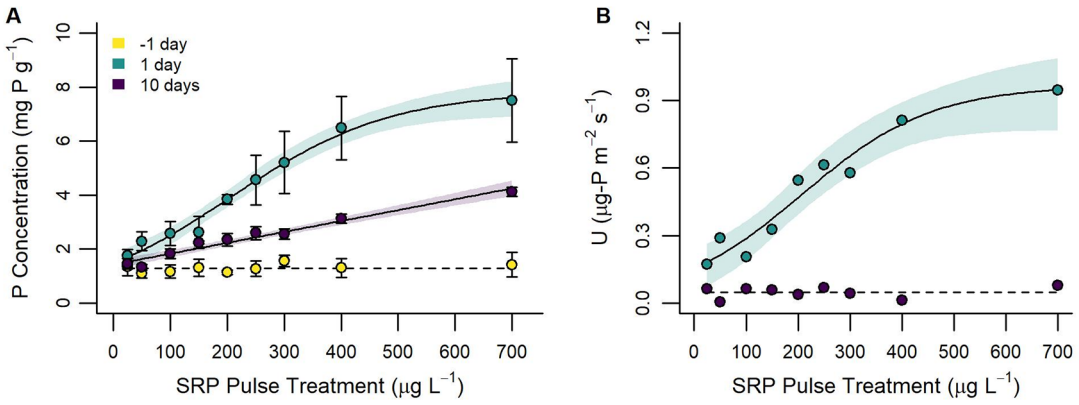

Figure 1. Periphyton P concentration (A) and periphyton P uptake (B) as functions of the experimental SRP gradient 1 day before (yellow), 1 day after (green), and 10 days after (purple) applying the 48-h SRP pulse treatment. Solid trend lines represent the fitted regression model with the strongest support and shaded areas indicate 95% confidence intervals. Dashed trend lines depict the null model. Error bars on observed points equal ±1 standard deviation from sample replicates (n = 3). Note: Data from the 1 day before time point represent ubiquitous pretreatment SRP concentrations (10 μg L^{-1}).

was taken to ensure that all peaks contributing to the signal within each region were integrated to allow for a quantitative comparison of compound classes between samples (Figure S3). However, assignment of a specific compound to most peaks was not attempted due to peak overlap, particularly in the monoester and diester regions, and the limited number of known compounds used as spikes.

Samples collected for periphyton biomass were frozen prior to analysis. Chlorophyll *a* (Chl *a*) was determined through hot ethanol extraction and fluorometric analysis.[15] Thawed samples were filtered onto Whatman GF/C filters and placed in 50 mL centrifuge tubes with 10 mL of 90% ethanol. Centrifuge tubes were partially submerged in a hot water bath at 80 °C for 7 min. Chl *a* concentration was determined from the liquid extract, which was diluted when necessary, with a Turner Designs Trilogy Fluorometer (Model: 7200−000). Ash-free dry-mass (AFDM) was determined through loss on ignition. Thawed samples were filtered onto preashed Whatman GF/C filter papers and dried at 105 °C for 24 h and weighed. Samples were then ashed in a muffle furnace at 500 °C for 1 h and subsequently weighed to determine the mass of organic matter lost on ignition.

2.4. Statistical Analyses. Null (intercept-only), linear, and nonlinear (i.e., asymptotic, and logistic) least-squares regression models were used to evaluate trends in each of periphyton P concentration, P speciation, P uptake, and biomass across the experimental SRP gradient for the three sampling events. Asymptotic and logistic regression models, common in algal growth and uptake kinetics,[63,64] were used to indicate if nonlinear growth models better predicted the association between periphyton and experimental SRP concentrations than linear models. Regression analyses were performed in R (version 3.6.1) with the *stats* package.

Null, linear, and nonlinear regression models were compared through Akaike's information criterion corrected for small samples size.[65] Models were evaluated based on AIC differences corrected for small sample size (AIC_c) where $\Delta AIC_c > 2$ indicated poor model support.[66] Relative likelihoods and AIC weights (AIC_w) were estimated to quantify the strength of support for each model and used to calculate evidence ratios.[67] These metrics were used to determine the model that was more likely when two or more models showed comparable support based on AIC_c ($\Delta AIC_c <$ 2). Adjusted R^2 (pseudoadjusted R^2 for nonlinear models) were reported for the models selected by AIC_c. AIC_c information were computed with the *bbmle* package in *R*.[68]

To evaluate the correspondence between observed periphyton biomass accrual and expected biomass accrual from assimilated P,[69] linear regression models were used to describe the ratio between periphyton P consumption relative to the biofilm P quota (independent) and the increase in periphyton biomass (dependent) from 1 to 10 days after applying the experimental SRP pulse treatment. Expected biomass accrual from assimilated P can be ascertained from the use of cellular P for replication. Cellular (algal and bacterial) replication requires a 2-fold increase in inorganic nutrient content relative to the cellular nutrient quota (i.e., minimum intracellular nutrient concentration) to support one cell doubling.[69] Thus, under optimal conditions, there should be an approximately 2:1 ratio between periphyton P consumption relative to the P quota of the biofilm and periphyton biomass accrual. Periphyton P consumption and biomass accrual was determined from the difference in the predicted values of regression models fitted 1 day and 10 days after applying the experimental SRP treatment. Percent biomass accrual was estimated as the percent increase in Chl *a* and AFDM 10 days after applying the experimental SRP treatment relative to the biomass 1 day after. In contrast, periphyton P consumption was estimated as the percent decrease in P content from 1 day to 10 days after applying the experimental SRP pulse treatment relative to the predicted P content 1 day before SRP addition. P content before experimental additions was used to represent the P quota of periphyton communities under ambient SRP concentrations (10 μg L^{-1} P).

3. RESULTS

3.1. Effect of SRP Pulse Concentration on Periphyton P Content. The day prior to 48-h SRP pulses, P concentration in periphyton biomass was 1.29 ± 0.15 mg P g^{-1} (mean ± standard deviation) (Figure 1). Regression model comparisons indicated unambiguous support ($\Delta AICc > 2$) for the null model (AIC_w = 0.73), indicating consistent periphyton P concentrations across experimental units prior to applying the SRP pulse treatment (Figure 1A; Table S2).

The P uptake rate of periphyton ranged from 0.17 to 0.95 μg-P m^{-2} s^{-1} during the SRP pulse and <0.01 to 0.08 μg-P m^{-2}

https://doi.org/10.1021/acs.est.2c06285
Environ. Sci. Technol. 2023, 57, 4643−4655

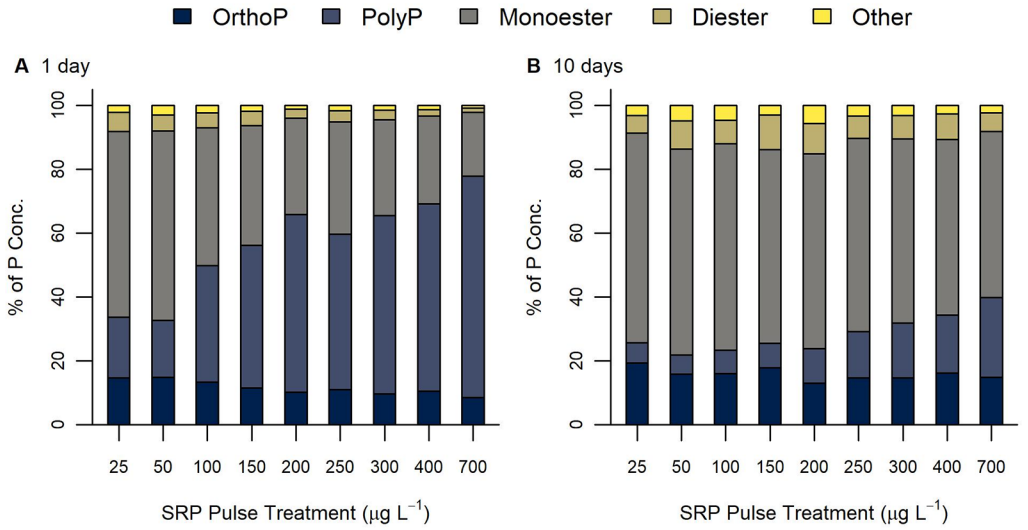

Figure 2. Composition of phosphorus content speciation (PolyP: polyphosphate, OrthoP: orthophosphate, Monoester: phospho-monoesters, Diester: phospho-diesters) as functions of the experimental SRP gradient (A) 1 day and (B) 10 days after applying the 48 h SRP pulse treatment.

s^{-1} after the reestablishment of ambient SRP concentrations (Figure 1B; Table S2). Regression model comparisons for P uptake during the pulse indicated support for positive logistic and linear models, but support for the logistic model (AICw = 0.49; pseudoadjusted R^2 = 0.93) was stronger than for the linear model (AICw = 0.36). P uptake approached an asymptote of about 0.95 μg-P m^{-2} s^{-1} at a SRP pulse concentration around 400 μg L^{-1}. Regression model comparisons for P uptake after the reestablishment of ambient SRP concentrations indicated unambiguous support (ΔAICc > 2) for the null model (AIC_w = 0.89) across SRP pulse treatments.

Periphyton P concentration increased 1.3 to 5.8-fold in association with the 15 to 690 μg L^{-1} increase in surface water SRP concentrations over the 48-h pulse (Figure 1A; Table S2). Regression model comparison identified unambiguous support (AIC_w = 0.97) for the logistic model between SRP pulse concentration and periphyton P concentration 1-day after the high concentration SRP pulse (pseudoadjusted R^2 = 0.98). Here, periphyton P concentration approached an asymptote of about 7.60 mg P g^{-1} or 0.76% dry weight between pulse concentrations of 400 and 700 μg L^{-1} SRP.

Ten days after the high concentration SRP pulse, periphyton P concentration had declined 1.2 to 2.1-fold from concentrations observed 1 day after the SRP pulse (Figure 1A; Table S2). However, periphyton P concentrations remained 1.0 to 3.2-fold greater 10 days after compared to prior to the SRP pulse. Regression model comparison indicated unambiguous support for a positive linear association between periphyton P concentration and streamwater SRP concentration (AIC_w = 0.73; adjusted R^2 = 0.96) 10 days after the SRP pulse.

3.2. Effect of SRP Pulse Concentration on Periphyton P Speciation. After applying the SRP pulse treatment, the relative contribution of individual P species to total periphyton P concentration varied across the experimentally imposed gradient of SRP concentrations (Figures 2 and S1). Periphyton P speciation 1 day after was dominated by polyphosphates (19−69% of total P) and phosphomonoesters (20−58%) with lower proportions of orthophosphate (9−15%), phosphodiester (1−6%), and other P species (1−3%). In contrast, periphyton P speciation 10 days after was dominated by phosphomonoesters (52−66%) with the relative proportion of polyphosphates (6−25%) decreasing in comparison to the previous time point. Orthophosphate (13−19%), phosphodiesters (5−11%), and other P species (2−6%) comprised smaller proportions of the total P content 10 days after applying the SRP pulse treatment.

Periphyton polyphosphate concentration 1 day after applying the SRP pulse treatment ranged from 0.3 to 5.2 mg P g^{-1} (Figure 3A). Regression model comparisons indicated near equal support for positive logistic (AIC_w = 0.48; pseudoadjusted R^2 = 0.98) and asymptotic (AIC_w = 0.40) models of polyphosphate concentration as a function of the SRP pulse treatment gradient. Periphyton polyphosphate concentration increased over the SRP concentration gradient and approached an asymptote of about 5.1 mg P g^{-1} between pulse concentrations of 400 and 700 μg L^{-1} SRP. Periphyton polyphosphate concentration decreased between samples collected 1 day and 10 days after the applying the SRP pulse across all artificial streams. However, the decrease in polyphosphate was greater in artificial streams that received higher concentration pulses. Ten days after applying the SRP pulse treatment, periphyton polyphosphate concentration ranged from 0.1 to 1.0 mg P g^{-1}, and there was unambiguous support for a positive linear association between polyphosphate and SRP pulse concentration (AIC_w = 0.91; adjusted R^2 = 0.99).

Periphyton orthophosphate concentration 1 day after the SRP pulse ranged from about 0.3 to 0.7 mg P g^{-1} with pulse concentrations (Figure 3B). Regression model comparisons indicated support for linear and logistic models. However, support for a positive linear (AICw = 0.65; adjusted R^2 = 0.74) association between periphyton orthophosphate concentration and SRP pulse concentration outweighed that of the logistic model (AICw = 0.24). Periphyton orthophosphate concentration 10 days after the SRP pulses (0.2 to 0.6 mg P g^{-1}) decreased about 1.2-fold in comparison to samples collected 1 day after. Regression model comparison indicated unambiguous support for a positive linear association between orthophosphate and SRP pulse concentration (AIC_w = 0.94; adjusted R^2 = 0.86) (Figure 3B).

https://doi.org/10.1021/acs.est.2c06285
Environ. Sci. Technol. 2023, 57, 4643−4655

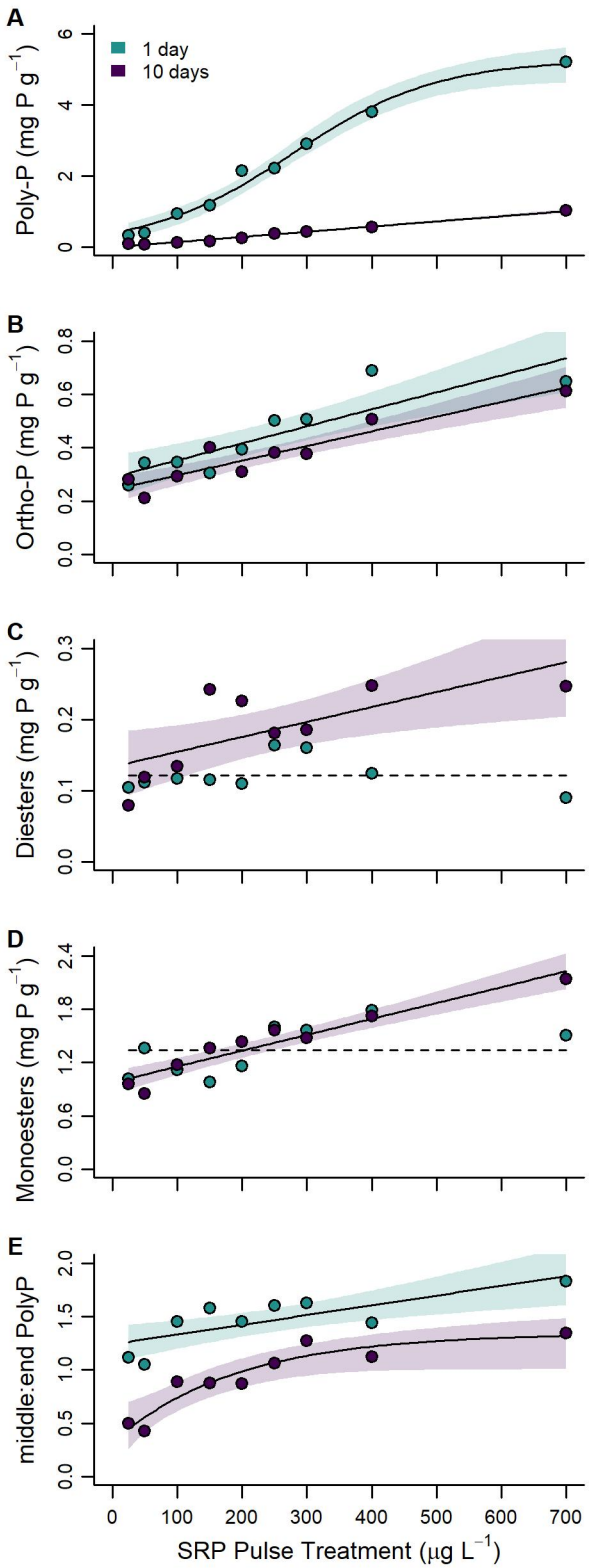

Figure 3. Periphyton (A) polyphosphate, (B) orthophosphate, (C) phospho-diesters, (D) phospho-monoesters, and (E) middle:end polyphosphate groups as functions of the experimental SRP gradient 1 day (green) and 10 days after (purple) applying the 48-h SRP pulse treatment. Solid trend lines represent the fitted regression model with the strongest support and shaded areas indicate 95% confidence intervals. Dashed trend lines depict the null model. Error bars on observed points equal ±1 standard deviation from sample replicates (n = 3).

In contrast, 1 day after applying the SRP pulse treatment periphyton phosphodiester concentrations (0.09 to 0.16 mg P g^{-1}) did not differ across the SRP pulse concentration gradient with unambiguous support for the null model (AICw = 0.91; Figure 3C). However, periphyton phosphodiester concentrations increased between samples collected 1-day and 10-days after the SRP pulses where artificial streams receiving higher concentration SRP pulses had periphyton with greater phosphodiester concentrations (0.08 to 0.25 mg P g^{-1}). There was support for null (AIC_w = 0.14), linear (AIC_w = 0.31), asymptotic (AIC_w = 0.27), and logistic (AIC_w = 0.28) models for periphyton phosphodiester concentration as a function of SRP pulse concentration 10 days after applying the SRP pulse treatment, but the positive linear model was most supported based on AIC_w evidence ratios (adjusted R^2 = 0.44) (Figure 3C).

Phosphomonoester concentrations (1.0 to 1.8 mg P g^{-1}) also did not differ as a function of the SRP pulse concentration gradient 1 day after applying the treatment (Figure 3D). Both null model (AIC_w = 0.53) and linear (AIC_w = 0.43) models were supported here, but the null model had the highest evidence ratio. Periphyton monoester concentrations did not differ greatly between samples collected 1-day and 10-days after SRP pulses (0.9 to 2.1 mg P g^{-1}); however, there was strong support for both positive linear (AIC_w = 0.60) and asymptotic (AIC_w = 0.28) models for periphyton phosphomonoester concentration as a function of SRP pulse concentrations 10 days after applying the SRP pulse treatment. The positive linear model fit was most strongly supported (adjusted R^2 = 0.90).

Length of polyphosphate chains, represented here by the ratio of polyphosphate end groups to polyphosphate middle groups,[55,56] was also associated with SRP pulse concentration both 1 and 10 days after applying the SRP pulse treatment (Figure 3E). Polyphosphate chain length ratios ranged from 1.05 to 1.83 and 0.42 to 1.34 along the SRP pulse concentration gradient for samples collected 1 day and 10 days after, respectively. For samples collected 1 day after experimental SRP additions, there was unambiguous support for a positive linear association (AIC_w = 0.61) between polyphosphate chain length ratio and SRP pulse concentration (adjusted R^2 = 0.55). In contrast, there was support for positive linear (AIC_w = 0.19), asymptotic (AIC_w = 0.48), and logistic (AIC_w = 0.33) associations between polyphosphate chain length ratio and SRP pulse concentration 10 days after. However, the asymptotic model had the strongest support and approached an asymptote at a middle:end polyphosphate group ratio of about 1.30 around 400 μg L^{-1} SRP (pseudoadjusted R^2 = 0.86). The polyphosphate chain length ratio decreased about 1.7-fold between samples collected 1 day and 10 days after the SRP pulses.

3.3. Effects of SRP Pulse Concentration on Periphyton Biomass. Periphyton biomass was on average (±standard deviation) 2.50 ± 0.79 μg Chl *a* cm^{-2} and 0.50 ± 0.08 mg AFDM cm^{-2} 1 day before the SRP pulses. There was unambiguous support that periphyton biomass was consistent (Chl *a*: AICw = 0.90; AFDM: AICw = 0.81) across artificial streams after acclimatization (Figure 4; Table S4).

The day after experimental SRP pulses periphyton biomass averaged 5.90 ± 0.74 μg Chl *a* cm^{-2} and 0.94 ± 0.16 mg AFDM cm^{-2}. This represents an approximate doubling of Chl *a* concentration and AFDM in all artificial streams in association with SRP pulse additions. Neither Chl *a* nor

https://doi.org/10.1021/acs.est.2c06285
Environ. Sci. Technol. 2023, 57, 4643−4655

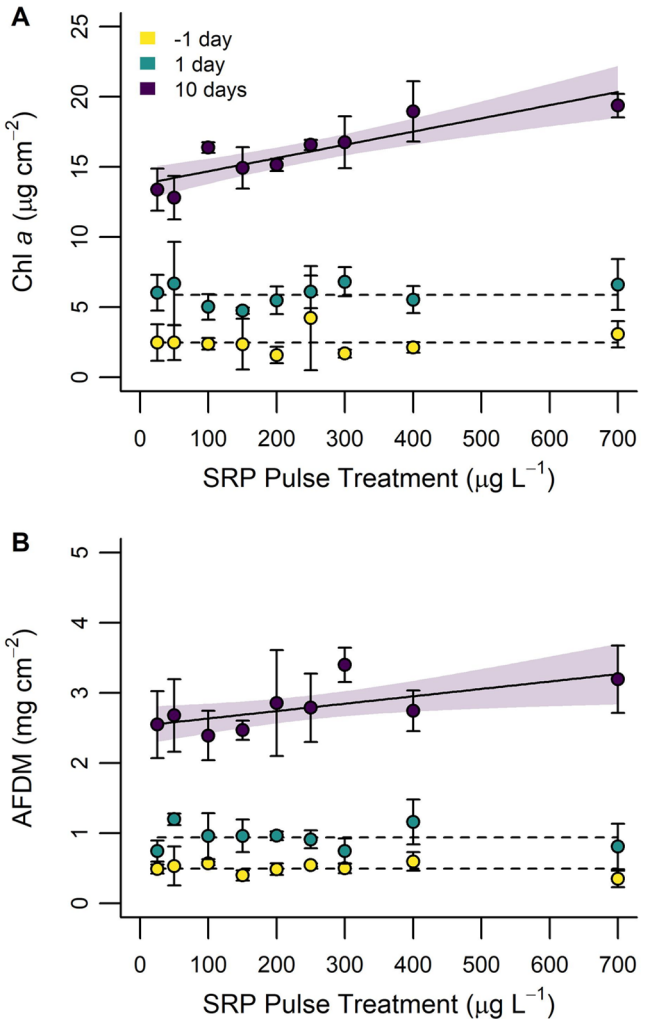

Figure 4. Periphyton biomass as measured by (A) chlorophyll *a* (Chl a) and (B) ash-free dry-mass (AFDM) as functions of the experimental SRP gradient 1 day before (yellow), 1 day after (green), and 10 days after (purple) applying the 48-h SRP pulse treatment. Trend lines represent the fitted regression model with the strongest support and shaded areas show 95% confidence intervals. Dashed trend lines depict the null model. Error bars on observed points equal ±1 standard deviation from sample replicates (n = 3). Note: Data from the 1 day before time point represent ubiquitous pretreatment SRP concentrations (10 μg L^{-1}).

AFDM were associated with SRP pulse concentration 1 day after as indicated by unambiguous support for null regression models (Chl *a*: AICw = 0.87; AFDM: AICw = 0.90) (Figure 4).

Ten days after SRP pulse additions, Chl *a* and AFDM had increased in all mesocosms and ranged from 12.81 to 19.38 μg Chl *a* cm^{-2} and 2.39 to 3.20 mg AFDM cm^{-2}, respectively. There was unambiguous support for a positive linear association between Chl *a* and SRP pulse concentration (AICw = 0.77; adjusted R^2 = 0.75) 10 days after SRP pulse additions. Similarly, a positive linear association between AFDM and SRP pulse concentration was supported (AICw = 0.55), and while the null (AICw = 0.42) model was also supported, the linear model was 1.3-fold more likely (adjusted R^2 = 0.37) (Figure 4).

3.4. Periphyton P Assimilation from SRP Pulses. Periphyton P concentrations decreased 1.2- to 2.1-fold between 1 day and 10 days after experimental SRP pulses, whereas periphyton biomass increased 2.1- to 3.6-fold over the same period. Fitted values from regression models (Figures 1A and 4) revealed that the periphyton P quota (i.e., the quantity of P taken up between 1 day before and 1 day after SRP pulsing) was associated (adjusted R^2 > 0.86) with the quantity of biomass accrued from 1 day to 10 days after experimental SRP pulses for both Chl a and AFDM. However, regression coefficients from these linear models indicated that the ratio between periphyton P consumption (relative to the biofilm P quota) and periphyton biomass accrual was 2.84:1 for Chl *a* and 4.05:1 for AFDM, about 30% and 51% higher than the optimal 2:1 ratio required for cell doubling[69] (Figure 5).

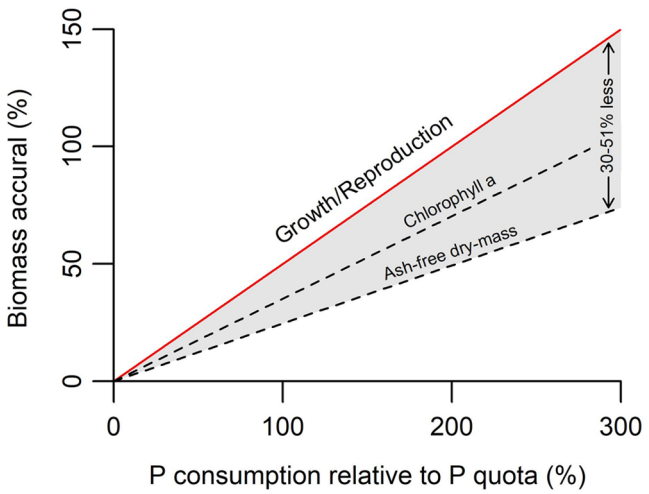

Figure 5. Difference between the theoretical (red line) association and observed (dashed lines) associations of phosphorus consumption (relative to the periphyton phosphorus quota) and biomass accrual from 1 day to 10 days after applying the experimental SRP pulse treatment.

4. DISCUSSION

P concentration in streams is rarely constant over time or as a function of flow. P exhibits highly variable concentration-discharge relationships dependent on multiple factors.[70,71] Therefore, many stream bed environments are exposed to periods of P abundance and scarcity even over short time periods of hours or days. Our study of periphyton P uptake during simulated short-duration, high concentration events after a period of low P concentration demonstrates that periphyton communities can respond rapidly to changes in surface water P concentration and are therefore well adapted to natural oscillations in P availability (Figure 6). Specifically, we observed that periphyton communities not only take up significant quantities of P beyond their immediate growth requirements during short periods of high SRP exposure, but they then sustain growth by assimilating stored P (i.e., polyphosphates) into P containing biomolecules (i.e., phospho-monoesters and phospho-diesters). Indeed, our study shows that a single high concentration, short duration event can sustain increased periphyton growth for at least 10 days. Further, we have elucidated an upper limit in the intracellular storage of P as polyphosphate and inefficiencies in its subsequent use in the production of functional biomass.

4.1. P Uptake by Biofilms. We observed that internal P concentration in periphyton increased by as much as 5.8-fold

https://doi.org/10.1021/acs.est.2c06285
Environ. Sci. Technol. 2023, 57, 4643−4655

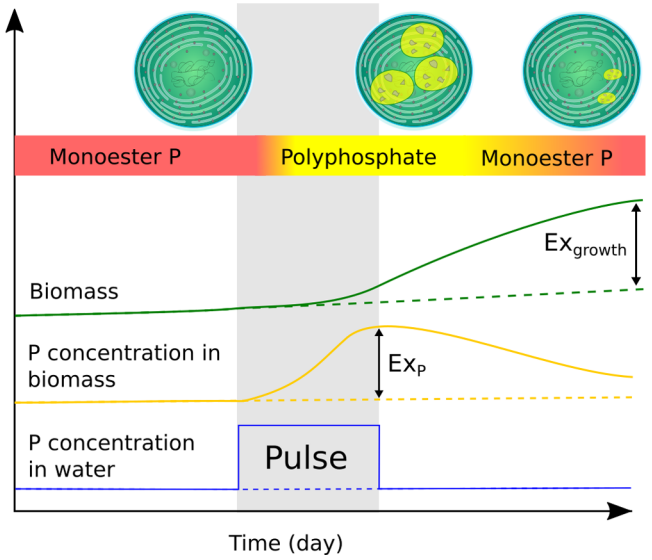

Figure 6. Solid lines indicate trends in periphyton biomass (green), dominant intracellular P species (colored horizontal bar), and biomass P concentration (yellow) in response to short increase in surface water SRP concentration (blue) marked "Pulse". Dashed lines indicate trajectories in the absence of an SRP pulse. P concentration within biomass increases dramatically during the pulse period due to the rapid accumulation of polyphosphate within cells but does not immediately result in rapid growth. Upon cessation of the pulse, P stored in cells results in increases to biomass beyond that which could be supported by surface water SRP concentrations alone. As biomass increases and intracellular polyphosphate stores become depleted after the pulse, phosphomonoesters return as the dominant P species.

after exposure to 48 h of elevated SRP concentrations in surface water, which equated to a maximum P uptake rate of 0.95 μg-P m^{-2} s^{-1}. This resulted in total P concentrations of up to 7.5 mg P g^{-1} periphyton dry weight and P uptake rates up to 20 times greater than those observed following the reestablishment of ambient SRP concentrations (i.e., 10 μg L^{-1}). SRP uptake rates did not vary as a function of SRP pulse concentration during the period after the pulse (Figure 1). This indicates that additional SRP was only retained by periphyton during the pulse period and not via uptake of SRP retained within the flumes via abiotic mechanisms (e.g., sorption or precipitation to cobbles or channel walls). The extent of uptake observed here highlights the potential for periphyton to mediate P concentrations and attenuate loads in low order streams during short duration, high concentration events at subscouring flows. Elevated internal P concentrations in periphyton have been reported in past mesocosm studies assessing short duration increases in streamwater P concentrations.[33,72−75] Moreover, our observed rates of P uptake are within the range of those observed in field studies[31,76−79] (e.g., 0.06−1.47 μg m^{-2} s^{-1}). However, we show that internal P storage and redistribution within periphyton in response to the short-term enrichment of SRP concentrations readily occurs in environments with sufficient ambient P availabilities.

Periphyton P uptake increased in a nonlinear fashion in response to the SRP concentration gradient, corroborating several prior studies on algal responses to increasing surface water P concentrations,[63,80−82] including those of short duration.[34] Our results thus reaffirm that there is an upper limit of P uptake by periphyton. However, our study identified an upper limit in periphyton P uptake corresponding to surface water SRP concentrations of approximately 400 μg L^{-1} SRP. This value is over an order of magnitude greater than saturation concentrations reported for periphyton growth at static P concentration[81] and is therefore strongly indicative of luxury P uptake in response to sudden increased P availability. While much higher than previously reported saturation concentrations, 400 μg L^{-1} SRP also falls within the range of concentrations commonly observed during high concentration events in streams exposed to agricultural and wastewater activities.[46−49] Therefore, representation of this upper limit may be required in mechanistic watershed models to accurately account for the role of periphyton luxury P uptake in response to sudden increase P availability in mediating P transport in streams. However, our study only varied SRP concentration in surface water and given that the synthesis of polyphosphate is energy intensive, the potential influence of other conditional factors (e.g., light availability and intracellular energy stores) in limiting P uptake rate during periods of P abundance remain uncertain.[83] Indeed, results from studies of enhanced biological P removal within wastewater treatment plants indicate that even greater uptake of P is physiologically possible (e.g., 380 mg P $g^{-1}_{\text{dry weight}}$; ref 3). Thus, P retention exceeding that observed in our study may be plausible in natural environments under more favorable environmental conditions where other constraints on P uptake rate are alleviated.

4.2. P Speciation. The proportion of polyphosphate, as well the polyphosphate chain length, was observed to increase in a nonlinear fashion along the SRP pulse concentration gradient. Moreover, polyphosphate became the dominant P species in periphyton at surface water SRP concentrations greater than 150 μg L^{-1} SRP. The increasing relative abundance of polyphosphate with surface water SRP concentration is consistent with luxury uptake since P in functional algal and bacterial biomass is normally dominated by P monoesters.[55,58] Although the concentration of orthophosphate was found to increase linearly with the SRP pulse concentration it is challenging to attribute this increase to a particular process or compound as numerous phosphate-containing compounds contribute signal to the orthophosphate peak observed in ^{31}P NMR spectra.[57]

Luxury uptake is a well described process in algae and bacteria,[34,35,43,83−85] particularly in environments with extremely high P and oscillating redox conditions, such as lake and marine sediments, as well as wastewater treatment facilities.[85,86] Recent studies have also reported that luxury uptake can occur in benthic stream environments where severe P limitation is prevalent.[33,87] The findings of our study extend our knowledge of luxury uptake in streams by demonstrating that (1) luxury uptake can occur even with sufficient ambient P availability under well oxygenated conditions; (2) there is an environmentally relevant upper limit to luxury P uptake; and (3) P-stores resulting from luxury uptake in periphyton can be substantial and likely modulate P spiralling in streams over a broad range of trophic status.

Our results indicate that P stored following luxury uptake (i.e., polyphosphate) during a 48-h high concentration SRP event was converted to functional P containing biomolecules (i.e., phospho-monoesters and phospho-diesters) over a period of several days following the reestablishment of ambient surface water SRP concentrations. Indeed, immediately following the event there was no relationship between the abundance of monoesters or diesters and the event concentration. However, after 10 days a strong positive, linear

https://doi.org/10.1021/acs.est.2c06285
Environ. Sci. Technol. 2023, 57, 4643−4655

relationship between event concentration and P-esters (i.e., phospho-monoesters and phospho-diesters) was observed coinciding with a marked decline in polyphosphate concentrations suggesting polyphosphate was partially converted to these functional P containing biomolecules during a period of increased growth (Figure S2). We did not attempt to quantify or correct for the often observed degradation of phospho-diesters, such as phospholipids and RNA, to phospho-monoesters during alkaline extraction and analysis by ^{31}P NMR.[59] Therefore, we do not report the phospho-monoester to phosphodiester ratios derived from our spectra. Greater amounts of the combined P-esters indicates that algal cells are in a more resource replete state to support growth.[88] We are unable to comment on the rate of polyphosphate conversion to P-esters during the 10 day post event period as we only obtained samples at two time points for analysis. However, polyphosphate stores were not completely depleted after 10 days with algal communities exposed to the high SRP pulse concentrations having about 10 times more polyphosphate than those exposed to low SRP pulse concentrations (Figure S2). The retention of polyphosphate for a period of 10 days indicates that polyphosphate stores may represent a useful P reservoir for growth for considerably longer than has been shown in previous studies.[89]

Further evidence for the conversion of polyphosphate into P-esters comes from the proportion of phosphate occurring in a terminal versus midchain position. Indeed, the proportion of polyphosphate groups occurring in the terminal position increased over the 10 day post pulse period indicating that the polyphosphate chain length is decreasing alongside P-ester production. This is consistent with the enzymatic hydrolysis of polyphosphate chains by exopolyphosphatases which are known to be processive, cleaving terminal phosphate groups.[90]

Periphyton biomass did not immediately respond to the addition of P from the high concentration event, but like P-ester concentrations, 10 days following the event periphyton biomass was linearly associated with the SRP concentration gradient. These relationships contrast with P uptake, which was nonlinear and exhibited an upper limit at 400 μg L^{-1} surface water P. Yet, this disparity may be potentially explained by the residual polyphosphate reserves that were particularly prevalent in periphyton above this upper limit and may represent unrealized P assimilation and growth potential during our experiment. Our observations support previous studies that have found that periphyton can utilize P loads from high concentration events to generate significant subsequent periphyton growth,[15,33,72,73] growth that has been posited to result in a mismatch between apparent low P concentration and high periphyton biomass.[11,91] This study contributes a unique perspective on the potential role and mechanism of polyphosphate storage and redistribution as explanation for this discrepancy. In the absence of a clear process for the internal storage and redistribution of P to support growth, the relative importance of flow event loading has not been fully recognized as an ecologically relevant source of P, nor implemented in process-based watershed nutrient models.

Based on our experimental results we were able to accurately determine P uptake rates by periphyton during high concentration events, but not the complete P mass balance, as not all P was retained in periphyton. Indeed, the amount of biomass produced after 10 days was about 30 to 51% less than would be expected from the use of P for cellular replication based on an increase of the P quota (sensu[69]). Several different explanations for this missing P are plausible. For example, Borchardt et al.,[92] reported that P leakage in replete algal cells (*Spirogyra fluviatilis*) was up to 3% of the P quota per hour immediately following a P pulse where rates of sustained (i.e., several hours) leakage were <1%. As such, leakage or loss in exudates could feasibly account for all missing P in our experiment. Alternatively, the rapid growth induced by P availability may have resulted in the sloughing of periphyton and downstream export of biomass and associated P, or stimulated grazing activity by benthic macroinvertebrates (secondary production). Quantifying each of these potential P redistribution mechanisms is thus necessary to determine the ultimate fate of P within the watershed.

It should be recognized that a variety of factors beyond P can limit periphyton growth.[93] The responses observed in our study represent those possible under environmental conditions conducive to growth (e.g., high light availability, warm temperatures, and stable flow). Many other factors (e.g., pulse duration, baseflow nutrient availability, flow velocity, cellular energy reserves, and periphyton community structure/composition) may influence the ecological potential of periphyton communities to assimilate P from short-duration, high concentration events.[87,93] Thus, although extensive efforts were taken to maximize realism of our artificial stream study, further research is needed to ascertain the controls and extent of the molecular mechanisms identified in our study in real-world streams.

4.3. Modeling and Management Implications. The rapid and extensive uptake of P observed in our experiment is conceptually consistent with the watershed hydrology literature. For example, lower magnitude flow events, particularly during warm periods, have been associated with anticlockwise P concentration-discharge hysteresis relationships indicating rapid P uptake from the water column.[94] In contrast, clockwise hysteresis behavior during events, whereby P concentration is higher during the rising limb than the falling limb of the hydrograph, has been attributed to mobilization and subsequent exhaustion of P accumulated in bed sediments.[95] Hysteresis behavior and P export also varies with antecedent conditions and event discharge, with longer dry periods and larger events resulting in more pronounced clockwise hysteresis and greater P transport.[94−96] Indeed, while the mobilization of bed sediments contributes to these observed trends, the preceding accumulation of P in periphyton and the subsequent scouring of this biomass may warrant further consideration in the estimation of riverine P loading.

Concentration-discharge relationships as they vary with hydrological conditions are starting to be used to improve accuracy of riverine P loading models (e.g., ref 97). However, our results indicate that the storage of P in periphyton biomass can occur far more rapidly during short-duration, high concentration events with subscouring flows than would occur under typical baseflow concentrations. Thus, we suggest that P accumulation by periphyton is unlikely to occur at a steady rate over time, but rather will vary as a function of P concentration during subscouring flows. Therefore, accounting for the number and magnitude of subscouring events with elevated P concentrations prior to a scouring event could improve loading estimates.

Our finding that stream biofilms are highly efficient at accumulating P under subscouring conditions also highlights

https://doi.org/10.1021/acs.est.2c06285
Environ. Sci. Technol. 2023, 57, 4643−4655

the importance of distinguishing between the P load contribution of land-to-channel and in-channel pools during scouring high flow events with which the majority of annual load is associated.[98] Indeed, the luxury uptake mechanism identified herein may also partially explain why inclusion of simple metrics of antecedent precipitation conditions into loading models do not always improve model accuracy.[97] While further work is required to determine the prevalence and relative importance of this mechanism in real streams, incorporating this conceptual understanding into river P loading models may enhance model predictions of individual event loads through a more sophisticated temporal representation of mobilizable P pools in river ecosystems.

5. CONCLUSIONS

There is increasing recognition that the complex biophysical processes in stream ecosystems result in transient retention of P, thus modulating the timing, speciation, and ultimate delivery of P to recipient downstream ecosystems. Here, we elucidated the biologically relevant P pools underpinning periphyton luxury P uptake during short duration, high concentration events. In doing so we have demonstrated that periphyton P uptake has the potential to (1) act as a buffer between edge of field P export and downstream waterbodies by decreasing peak loads in subscouring events; (2) delay P delivery to downstream waterbodies; (3) modify the speciation of the P load from dissolved P to particulate that can be more easily transferred to higher trophic levels and/or deposited into sediments. The underappreciated extent to which stream biofilms can contribute to transient P retention during episodic P loading events highlights an opportunity to improve management of P flows through watersheds and enhance the predictive capacity of watershed nutrient models.

■ ASSOCIATED CONTENT

Data Availability Statement

Data is available upon reasonable request.

Supporting Information

The Supporting Information is available free of charge at https://pubs.acs.org/doi/10.1021/acs.est.2c06285.

Example P NMR spectra and additional details on statistical model results (PDF)

■ AUTHOR INFORMATION

Corresponding Author

Nolan J. T. Pearce − *University of Western Ontario & Canadian Rivers Institute, London, Ontario N6A 3K8, Canada;* Present Address: Department of Biology, Trent University, 1600 W Bank Drive, Peterborough, Ontario, K9J 7B8, Canada; orcid.org/0000-0001-6600-5275; Email: nolanpearce@trentu.ca

Authors

Chris T. Parsons − *Ecohydrology Research Group and The Water Institute, University of Waterloo, Waterloo, Ontario N2L 3G1, Canada; Watershed Hydrology and Ecology Research Division, Environment and Climate Change Canada, Burlington, Ontario L7S 1A1, Canada;* orcid.org/0000-0002-6003-7716

Sarah M. Pomfret − *University of Western Ontario & Canadian Rivers Institute, London, Ontario N6A 3K8, Canada;* Present Address: Environmental Science and Technology Laboratories, Environment and Climate Change Canada, 867 Lakeshore Road, Burlington, Ontario, L7S 1A1, Canada

Adam G. Yates − *University of Western Ontario & Canadian Rivers Institute, London, Ontario N6A 3K8, Canada;* Present Address: Department of Biology, University of Waterloo, 200 University Avenue West, Waterloo, Ontario, N2L 3G1, Canada

Complete contact information is available at: https://pubs.acs.org/10.1021/acs.est.2c06285

Author Contributions

Conceptualization: N.J.T.P., C.T.P., A.G.Y.; Methodology: C.T.P., S.M.P.; Validation: C.T.P., S.M.P.; Software: N.J.T.P.; Investigation: N.J.T.P., S.M.P.; Formal Analysis: N.J.T.P., C.T.P.; Visualization: N.J.T.P., C.T.P.; Supervision: A.G.Y.; Resources: A.G.Y., C.T.P.; Project Administration: A.G.Y.; Funding Acquisition: A.G.Y., C.T.P.; Writing—original draft: N.J.T.P.; Writing—review and editing: N.J.T.P., A.G.Y., C.T.P.

Funding

Funding to Parsons from the Canada-Ontario Agreement on Great Lakes Water Quality and Ecosystem Health (ID 1306 16/17) and NSERC Discovery and NSERC PGS D

Notes

The authors declare no competing financial interest.

■ ACKNOWLEDGMENTS

Philippe Van Cappellen loan of lab space. Marianne Vandergriendt, Janet Venne, and Amanda Niederkorn assisted with the laboratory work. Erika Hill for assistance at TRESS. Patricia Chambers for helpful comments on an earlier version of the manuscript.

■ REFERENCES

(1) Cordell, D.; Drangert, J. O.; White, S. The Story of Phosphorus: Global Food Security and Food for Thought. *Global Environmental Change* **2009**, *19* (2), 292−305.

(2) Cordell, D.; White, S. Life's Bottleneck: Sustaining the World's Phosphorus for a Food Secure Future. *Annu. Rev. Environ. Resour* **2014**, *39*, 161−188.

(3) Zhang, C.; Guisasola, A.; Baeza, J. A. A Review on the Integration of Mainstream P-Recovery Strategies with Enhanced Biological Phosphorus Removal. *Water Res.* **2022**, *212*, 118102.

(4) Seitzinger, S. P.; Mayorga, E.; Bouwman, A. F.; Kroeze, C.; Beusen, A. H. W.; Billen, G.; van Drecht, G.; Dumont, E.; Fekete, B. M.; Garnier, J.; Harrison, J. A. Global River Nutrient Export: A Scenario Analysis of Past and Future Trends. *Global Biogeochem Cycles* **2010**, *24* (4), GB0A08.

(5) Baker, D. B.; Confesor, R.; Ewing, D. E.; Johnson, L. T.; Kramer, J. W.; Merryfield, B. J. Phosphorus Loading to Lake Erie from the Maumee, Sandusky and Cuyahoga Rivers: The Importance of Bioavailability. *J. Great Lakes Res.* **2014**, *40* (3), 502−517.

(6) Jarvie, H. P.; Johnson, L. T.; Sharpley, A. N.; Smith, D. R.; Baker, D. B.; Bruulsema, T. W.; Confesor, R. Increased Soluble Phosphorus Loads to Lake Erie: Unintended Consequences of Conservation Practices? *J. Environ. Qual* **2017**, *46* (1), 123−132.

(7) Schindler, D. W.; Carpenter, S. R.; Chapra, S. C.; Hecky, R. E.; Orihel, D. M. Reducing Phosphorus to Curb Lake Eutrophication Is a Success. *Environ. Sci. Technol.* **2016**, *50* (17), 8923−8929.

(8) Paerl, H. W.; Scott, J. T.; McCarthy, M. J.; Newell, S. E.; Gardner, W. S.; Havens, K. E.; Hoffman, D. K.; Wilhelm, S. W.; Wurtsbaugh, W. A. It Takes Two to Tango: When and Where Dual Nutrient (N & P) Reductions Are Needed to Protect Lakes and Downstream Ecosystems. *Environ. Sci. Technol.* **2016**, *50* (20), 10805−10813.

(9) Meyer, J. L.; Likens, G. E. Transport and Transformation of Phosphorus in a Forest Stream Ecosystem. *Ecology* **1979**, *60* (6), 1255−1269.
(10) de Klein, J. J. M.; Koelmans, A. A. Quantifying Seasonal Export and Retention of Nutrients in West European Lowland Rivers at Catchment Scale. *Hydrol Process* **2011**, *25* (13), 2102−2111.
(11) Jarvie, H. P.; Sharpley, A. N.; Scott, J. T.; Haggard, B. E.; Bowes, M. J.; Massey, L. B. Within-River Phosphorus Retention: Accounting for a Missing Piece in the Watershed Phosphorus Puzzle. *Environ. Sci. Technol.* **2012**, *46*, 13284−13292.
(12) Kao, N.; Mohamed, M.; Sorichetti, R. J.; Niederkorn, A.; van Cappellen, P.; Parsons, C. T. Phosphorus Retention and Transformation in a Dammed Reservoir of the Thames River, Ontario: Impacts on Phosphorus Load and Speciation. *J. Great Lakes Res.* **2022**, *48* (1), 84−96.
(13) Withers, P. J. A.; Jarvie, H. P. Delivery and Cycling of Phosphorus in Rivers: A Review. *Science of The Total Environment* **2008**, *400* (1−3), 379−395.
(14) Stutter, M. I.; Demars, B. O. L.; Langan, S. J. River Phosphorus Cycling: Separating Biotic and Abiotic Uptake during Short-Term Changes in Sewage Effluent Loading. *Water Res.* **2010**, *44* (15), 4425−4436.
(15) Pearce, N. J. T.; Thomas, K. E.; Lavoie, I.; Chambers, P. A.; Yates, A. G. Episodic Loadings of Phosphorus Influence Growth and Composition of Benthic Algae Communities in Artificial Stream Mesocosms. *Water Res.* **2020**, *185*, 116139.
(16) Small, G. E.; Ardón, M.; Duff, J. H.; Jackman, A. P.; Ramírez, A.; Triska, F. J.; Pringle, C. M. Phosphorus Retention in a Lowland Neotropical Stream Following an Eight-Year Enrichment Experiment. *Freshwater Science* **2016**, *35* (1), 1−11.
(17) Griffiths, N. A.; Johnson, L. T. Influence of Dual Nitrogen and Phosphorus Additions on Nutrient Uptake and Saturation Kinetics in a Forested Headwater Stream. *Freshwater Science* **2018**, *37* (4), 810−825.
(18) McDowell, R. W. Relationship between Sediment Chemistry, Equilibrium Phosphorus Concentrations, and Phosphorus Concentrations at Baseflow in Rivers of the New Zealand National River Water Quality Network. *J. Environ. Qual* **2015**, *44* (3), 921−929.
(19) Sharpley, A.; Jarvie, H. P.; Buda, A.; May, L.; Spears, B.; Kleinman, P. Phosphorus Legacy: Overcoming the Effects of Past Management Practices to Mitigate Future Water Quality Impairment. *J. Environ. Qual* **2013**, *42* (5), 1308−1326.
(20) Casillas-Ituarte, N. N.; Sawyer, A. H.; Danner, K. M.; King, K. W.; Covault, A. J. Internal Phosphorus Storage in Two Headwater Agricultural Streams in the Lake Erie Basin. *Environ. Sci. Technol.* **2020**, *54*, 176.
(21) Kusmer, A. S.; Goyette, J. O.; MacDonald, G. K.; Bennett, E. M.; Maranger, R.; Withers, P. J. A. Watershed Buffering of Legacy Phosphorus Pressure at a Regional Scale: A Comparison Across Space and Time. *Ecosystems* **2019**, *22* (1), 91−109.
(22) Froelich, P. N. Kinetic Control of Dissolved Phosphate in Natural Rivers and Estuaries: A Primer on the Phosphate Buffer Mechanism. *Limnol Oceanogr* **1988**, *33*, 649−668.
(23) Simpson, Z. P.; McDowell, R. W.; Condron, L. M.; McDaniel, M. D.; Jarvie, H. P.; Abell, J. M. Sediment Phosphorus Buffering in Streams at Baseflow: A Meta-Analysis. *J. Environ. Qual* **2021**, *50* (2), 287−311.
(24) Wang, Z.; Zhang, T.; Tan, C. S.; Qi, Z. Modeling of Phosphorus Loss from Field to Watershed: A Review. *J. Environ. Qual* **2020**, *49* (5), 1203−1224.
(25) Basu, N. B.; Destouni, G.; Jawitz, J. W.; Thompson, S. E.; Loukinova, N. v.; Darracq, A.; Zanardo, S.; Yaeger, M.; Sivapalan, M.; Rinaldo, A.; Rao, P. S. C. Nutrient Loads Exported from Managed Catchments Reveal Emergent Biogeochemical Stationarity. *Geophys. Res. Lett.* **2010**, *37* (23), L23404.
(26) Wironen, M. B.; Bennett, E. M.; Erickson, J. D. Phosphorus Flows and Legacy Accumulation in an Animal-Dominated Agricultural Region from 1925 to 2012. *Global Environmental Change* **2018**, *50* (March), 88−99.
(27) van Staden, T. L.; van Meter, K. J.; Basu, N. B.; Parsons, C. T.; Akbarzadeh, Z.; van Cappellen, P. Agricultural Phosphorus Surplus Trajectories for Ontario, Canada (1961−2016), and Erosional Export Risk. *Sci. Total Environ.* **2022**, *818*, 151717.
(28) van Meter, K. J.; McLeod, M. M.; Liu, J.; Tenkouano, G. T.; Hall, R. I.; van Cappellen, P.; Basu, N. B. Beyond the Mass Balance: Watershed Phosphorus Legacies and the Evolution of the Current Water Quality Policy Challenge. *Water Resour Res.* **2021**, *57* (10), 1−22.
(29) Williams, A.S.; Mushet, D.M.; Lang, M.; McCarty, G.W.; Shaffer, J.A.; Kahara, S. N.; Johnson, M.-V.V.; Kiniry, J.R. Improving the Ability to Include Freshwater Wetland Plants in Process-Based Models. *J. Soil Water Conserv* **2020**, *75* (6), 704−712.
(30) McDowell, R. W.; Noble, A.; Pletnyakov, P.; Haggard, B. E.; Mosley, L. M. Global Mapping of Freshwater Nutrient Enrichment and Periphyton Growth Potential. *Sci. Rep* **2020**, *10* (1), 1−13.
(31) Dodds, W. K. The Role of Periphyton in Phosphours Retention in Shallow Freshwater Aquatic Systems. *J. Phycol* **2003**, *39* (5), 840−849.
(32) Michalak, A. M.; Anderson, E. J.; Beletsky, D.; Boland, S.; Bosch, N. S.; Bridgeman, T. B.; Chaffin, J. D.; Cho, K.; Confesor, R.; Daloglu, I.; DePinto, J. v.; Evans, M. A.; Fahnenstiel, G. L.; He, L.; Ho, J. C.; Jenkins, L.; Johengen, T. H.; Kuo, K. C.; LaPorte, E.; Liu, X.; McWilliams, M. R.; Moore, M. R.; Posselt, D. J.; Richards, R. P.; Scavia, D.; Steiner, A. L.; Verhamme, E.; Wright, D. M.; Zagorski, M. A. Record-Setting Algal Bloom in Lake Erie Caused by Agricultural and Meteorological Trends Consistent with Expected Future Conditions. *Proc. Natl. Acad. Sci. U. S. A.* **2013**, *110* (16), 6448−6452.
(33) Rier, S. T.; Kinek, K. C.; Hay, S. E.; Francoeur, S. N. Polyphosphate Plays a Vital Role in the Phosphorus Dynamics of Stream Periphyton. *Freshwater Science* **2016**, *35* (2), 490−502.
(34) Solovchenko, A.; Khozin-Goldberg, I.; Selyakh, I.; Semenova, L.; Ismagulova, T.; Lukyanov, A.; Mamedov, I.; Vinogradova, E.; Karpova, O.; Konyukhov, I.; Vasilieva, S.; Mojzes, P.; Dijkema, C.; Vecherskaya, M.; Zvyagin, I.; Nedbal, L.; Gorelova, O. Phosphorus Starvation and Luxury Uptake in Green Microalgae Revisited. *Algal Res.* **2019**, *43*, 101651.
(35) Solovchenko, A. E.; Ismagulova, T. T.; Lukyanov, A. A.; Vasilieva, S. G.; Konyukhov, I. v.; Pogosyan, S. I.; Lobakova, E. S.; Gorelova, O. A. Luxury Phosphorus Uptake in Microalgae. *J. Appl. Phycol* **2019**, *31* (5), 2755−2770.
(36) Li, J.; Plouchart, D.; Zastepa, A.; Dittrich, M. Picoplankton Accumulate and Recycle Polyphosphate to Support High Primary Productivity in Coastal Lake Ontario. *Sci. Rep* **2019**, *9* (1), 1−10.
(37) Pearce, N. J. T.; Larson, J. H.; Evans, M. A.; Frost, P. C.; Xenopoulos, M. A. Episodic Nutrient Addition Affects Water Column Nutrient Processing Rates in River-to-Lake Transitional Zones. *J. Geophys Res. Biogeosci* **2021**, *126* (11), 1−16.
(38) Peterson, S. B.; Warnecke, F.; Madejska, J.; McMahon, K. D.; Hugenholtz, P. Environmental Distribution and Population Biology of Candidatus Accumulibacter, a Primary Agent of Biological Phosphorus Removal. *Environ. Microbiol* **2008**, *10* (10), 2692−2703.
(39) McMahon, K. D.; Read, E. K. Microbial Contributions to Phosphorus Cycling in Eutrophic Lakes and Wastewater. *Annu. Rev. Microbiol.* **2013**, *67*, 199−219.
(40) Lohman, K.; Priscu, J. C. Physiological Indicators of Nutrient Deficiency in Cladophora (Chlorophyta) in Clark Frok of the Columbia River, Montana. *J. Phycol* **1992**, *28*, 443−448.
(41) Stevenson, R. J.; Stoermer, E. F. Luxury Consumption of Phosphorus by Five Cladophora Epiphytes in Lake Huron. *Trans Am. Microsc Soc.* **1982**, *101* (2), 151−161.
(42) Havens, K. E.; East, T. L.; Rodusky, A. J.; Sharfstein, B. Littoral Periphyton Responses to Nitrogen and Phosphorus: An Experimental Study in a Subtropical Lake. *Aquat Bot* **1999**, *63* (3−4), 267−290.
(43) Saia, S. M.; Carrick, H. J.; Buda, A. R.; Regan, J. M.; Walter, M. T. Critical Review of Polyphosphate and Polyphosphate Accumulating Organisms for Agricultural Water Quality Management. *Environ. Sci. Technol.* **2021**, *55* (5), 2722−2742.

https://doi.org/10.1021/acs.est.2c06285
Environ. Sci. Technol. 2023, 57, 4643−4655

(44) Chambers, P. A.; McGoldrick, D. J.; Brua, R. B.; Vis, C.; Culp, J. M.; Benoy, G. A. Development of Environmental Thresholds for Nitrogen and Phosphorus in Streams. *J. Environ. Qual* **2012**, *41* (1), 7−20.
(45) Jarvie, H. P.; Smith, D. R.; Norton, L. R.; Edwards, F. K.; Bowes, M. J.; King, S. M.; Scarlett, P.; Davies, S.; Dils, R. M.; Bachiller-Jareno, N. Phosphorus and Nitrogen Limitation and Impairment of Headwater Streams Relative to Rivers in Great Britain: A National Perspective on Eutrophication. *Science of The Total Environment* **2018**, *621*, 849−862.
(46) Raney, S. M.; Eimers, M. C. Unexpected Declines in Stream Phosphorus Concentrations across Southern Ontario. *Canadian Journal of Fisheries and Aquatic Sciences* **2014**, *71* (3), 337−342.
(47) DeBues, M. J.; Eimers, M. C.; Watmough, S. A.; Mohamed, M. N.; Mueller, J. Stream Nutrient and Agricultural Land-Use Trends from 1971 to 2010 in Lake Ontario Tributaries. *J. Great Lakes Res.* **2019**, *45* (4), 752−761.
(48) Ontario Ministry of the Environment. *Water Quality of 15 Streams in Agricultural Watersheds of Southwestern Ontario 2004−2009*; 2012.
(49) Williams, M. R.; Livingston, S. J.; Penn, C. J.; Smith, D. R.; King, K. W.; Huang, C.-h. Controls of Event-Based Nutrient Transport within Nested Headwater Agricultural Watersheds of the Western Lake Erie Basin. *J. Hydrol (Amst)* **2018**, *559*, 749−761.
(50) Aspila, K. I.; Agemian, H.; Chau, A. S. Y. A Semi-Automated Method for the Determination of Inorganic, Organic and Total Phosphate in Sediments. *Analyst* **1976**, *101* (1200), 187−197.
(51) Cade-Menun, B. J. Improved Peak Identification in 31P-NMR Spectra of Environmental Samples with a Standardized Method and Peak Library. *Geoderma* **2015**, *257−258*, 102−114.
(52) Cade-Menun, B. J.; Liu, C. W.; Nunlist, R.; McColl, J. G. Soil and Litter Phosphorus-31 Nuclear Magnetic Resonance Spectroscopy. *J. Environ. Qual* **2002**, *31* (2), 457−465.
(53) Parsons, C. T.; Rezanezhad, F.; O'Connell, D. W.; van Cappellen, P. Sediment Phosphorus Speciation and Mobility under Dynamic Redox Conditions. *Biogeosciences* **2017**, *14* (14), 3585−3602.
(54) Shinohara, R.; Ouellette, L.; Nowell, P.; Parsons, C. T.; Matsuzaki, S.-i. S.; Paul Voroney, R. The Composition of Particulate Phosphorus: A Case Study of the Grand River, Canada. *J. Great Lakes Res.* **2018**, *44* (3), 527−534.
(55) Wang, L.; Kuchendorf, C.; Willbold, S. Determination of Individual Chain Length and Chain-Length Distribution of Polyphosphates in Microalgae by 31P-DOSY-NMR. *Algal Res.* **2019**, *43*, 101631.
(56) Christ, J. J.; Willbold, S.; Blank, L. M. Methods for the Analysis of Polyphosphate in the Life Sciences. *Anal. Chem.* **2020**, *92* (6), 4167−4176.
(57) Cade-Menun, B. J.; Navaratnam, J. A.; Walbridge, M. R. Characterizing Dissolved and Particulate Phosphorus in Water with 31P Nuclear Magnetic Resonance Spectroscopy. *Environ. Sci. Technol.* **2006**, *40* (24), 7874−7880.
(58) Feng, W.; Zhu, Y.; Wu, F.; Meng, W.; Giesy, J. P.; He, Z.; Song, L.; Fan, M. Characterization of Phosphorus Forms in Lake Macrophytes and Algae by Solution 31P Nuclear Magnetic Resonance Spectroscopy. *Environmental Science and Pollution Research* **2016**, *23* (8), 7288−7297.
(59) Cade-Menun, B.; Liu, C. W. Solution Phosphorus-31 Nuclear Magnetic Resonance Spectroscopy of Soils from 2005 to 2013: A Review of Sample Preparation and Experimental Parameters. *Soil Science Society of America Journal* **2014**, *78* (1), 19−37.
(60) McDowell, R. W.; Stewart, I. The Phosphorus Composition of Contrasting Soils in Pastoral, Native and Forest Management in Otago, New Zealand: Sequential Extraction and 31P NMR. *Geoderma* **2006**, *130* (1−2), 176−189.
(61) Wojdyr, M. Fityk: A General-Purpose Peak Fitting Program. *J. Appl. Crystallogr.* **2010**, *43* (5), 1126−1128.
(62) Turner, B. L.; Mahieu, N.; Condron, L. M. Phosphorus-31 Nuclear Magnetic Resonance Spectral Assignments of Phosphorus Compounds in Soil NaOH-EDTA Extracts. *Soil Science Society of America Journal* **2003**, *67* (2), 497−510.
(63) Dodds, W. K.; Clements, W. H.; Gido, K.; Hilderbrand, R. H.; King, R. S. Thresholds, Breakpoints, and Nonlinearity in Freshwaters as Related to Management. *J. North Am. Benthol Soc.* **2010**, *29* (3), 988−997.
(64) Lee, E.; Jalalizadeh, M.; Zhang, Q. Growth Kinetic Models for Microalgae Cultivation: A Review. *Algal Res.* **2015**, *12*, 497−512.
(65) Burnham, K. P.; Anderson, D. R. Multimodel Inference: Understanding AIC and BIC in Model Selection. *Sociol Methods Res.* **2004**, *33* (2), 261−304.
(66) Burnham, K. P.; Anderson, D. R.; Huyvaert, K. P. AIC Model Selection and Multimodel Inference in Behavioral Ecology: Some Background, Observations, and Comparisons. *Behav Ecol Sociobiol* **2011**, *65* (1), 23−35.
(67) Wagenmakers, E. J.; Farrell, S. AIC Model Selection Using Akaike Weights. *Psychon Bull. Rev.* **2004**, *11* (1), 192−196.
(68) Bolker, B.; Gine-Vazque, I. *Bbmle: Tools for General Maximum Likelihood Estimation*; 2020.
(69) Sabater, S.; Artigas, J.; Corcoll, N.; Proia, L.; Timoner, X.; Tornes, E. Ecophysiology of River Algae. In *River Algae*; Necchi, O., Jr., Ed.; Springer: Cham, 2016; pp 197−218.
(70) Pohle, I.; Baggaley, N.; Palarea-Albaladejo, J.; Stutter, M.; Glendell, M. A Framework for Assessing Concentration-Discharge Catchment Behavior From Low-Frequency Water Quality Data. *Water Resour Res.* **2021**, *57* (9), e2021WR029692.
(71) Rattan, K. J.; Bowes, M. J.; Yates, A. G.; Culp, J. M.; Chambers, P. A. Evaluating Diffuse and Point Source Phosphorus Inputs to Streams in a Cold Climate Region Using a Load Apportionment Model. *J. Great Lakes Res.* **2021**, *47* (3), 761−772.
(72) Humphrey, K. P.; Stevenson, R. J. Responses of Benthic Algae to Pulses in Current and Nutrients during Simulations of Subscouring Spates. *J. North Am. Benthol Soc.* **1992**, *11* (1), 37−48.
(73) Davies, J.; Bothwell, M. L. Responses of Lotic Periphyton to Pulses of Phosphorus: P-Flux Controlled Growth Rate. *Freshw Biol.* **2012**, *57* (12), 2602−2612.
(74) Song, C.; Søndergaard, M.; Cao, X.; Zhou, Y. Nutrient Utilization Strategies of Algae and Bacteria after the Termination of Nutrient Amendment with Different Phosphorus Dosage: A Mesocosm Case. *Geomicrobiol J.* **2018**, *35* (4), 294−299.
(75) Santos, S. A. M.; dos Santos, T. R.; Furtado, M. S. R.; Henry, R.; Ferragut, C. Periphyton Nutrient Content, Biomass and Algal Community on Artificial Substrate: Response to Experimental Nutrient Enrichment and the Effect of Its Interruption in a Tropical Reservoir. *Limnology (Tokyo)* **2018**, *19* (2), 209−218.
(76) Niyogi, D. K.; Simon, K. S.; Townsend, C. R. Land Use and Stream Ecosystem Functioning: Nutrient Uptake in Streams That Contrast in Agricultural Development. *Arch Hydrobiol* **2004**, *160* (4), 471−486.
(77) Weigelhofer, G.; Ramião, J. P.; Puritscher, A.; Hein, T. How Do Chronic Nutrient Loading and the Duration of Nutrient Pulses Affect Nutrient Uptake in Headwater Streams. *Biogeochemistry* **2018**, *141* (2), 249−263.
(78) Weigelhofer, G. The Potential of Agricultural Headwater Streams to Retain Soluble Reactive Phosphorus. *Hydrobiologia* **2017**, *793*, 149.
(79) Ensign, S. H.; Doyle, M. W. Nutrient Spiraling in Streams and River Networks. *J. Geophys Res. Biogeosci* **2006**, *111* (4), 1−13.
(80) Taylor, J. M.; King, R. S.; Pease, A. A.; Winemiller, K. O. Nonlinear Response of Stream Ecosystem Structure to Low-Level Phosphorus Enrichment. *Freshw Biol.* **2014**, *59* (5), 969−984.
(81) Schmidt, T. S.; Konrad, C. P.; Miller, J. L.; Whitlock, S. D.; Stricker, C. A. Benthic Algal (Periphyton) Growth Rates in Response to Nitrogen and Phosphorus: Parameter Estimation for Water Quality Models. *J. Am. Water Resour Assoc* **2019**, *55* (6), 1479−1491.
(82) Price, K. J.; Carrick, H. J. Effects of Experimental Nutrient Loading on Phosphorus Uptake by Biofilms: Evidence for Nutrient Saturation in Mid-Atlantic Streams. *Freshwater Science* **2016**, *35* (2), 503−517.

https://doi.org/10.1021/acs.est.2c06285
Environ. Sci. Technol. 2023, 57, 4643−4655

(83) Sanz-Luque, E.; Bhaya, D.; Grossman, A. R. Polyphosphate: A Multifunctional Metabolite in Cyanobacteria and Algae. *Front Plant Sci.* **2020**, *11* (June), 1−21.
(84) Hupfer, M.; Glöss, S.; Schmieder, P.; Grossart, H. P. Methods for Detection and Quantification of Polyphosphate and Polyphosphate Accumulating Microorganisms in Aquatic Sediments. *Int. Rev. Hydrobiol* **2008**, *93* (1), 1−30.
(85) Wang, D.; Li, Y.; Cope, H. A.; Li, X.; He, P.; Liu, C.; Li, G.; Rahman, S. M.; Tooker, N. B.; Bott, C. B.; Onnis-Hayden, A.; Singh, J.; Elfick, A.; Marques, R.; Jessen, H. J.; Oehmen, A.; Gu, A. Z. Intracellular Polyphosphate Length Characterization in Polyphosphate Accumulating Microorganisms (PAOs): Implications in PAO Phenotypic Diversity and Enhanced Biological Phosphorus Removal Performance. *Water Res.* **2021**, *206*, 117726.
(86) Saia, S. M.; Sullivan, P. J.; Regan, J. M.; Carrick, H. J.; Buda, A. R.; Locke, N. A.; Walter, M. T. Evidence for Polyphosphate Accumulating Organism (PAO)-Mediated Phosphorus Cycling in Stream Biofilms under Alternating Aerobic/Anaerobic Conditions. *Freshwater Science* **2017**, *36* (2), 284−296.
(87) Taylor, S.; Saia, S. M.; Buda, A. R.; Regan, J. M.; Walter, M. T.; Carrick, H. J. Polyphosphate Accumulation Tracks Incremental P-Enrichment in a Temperate Watershed (Pennsylvania, United States) as an Indicator of Stream Ecosystem Legacy P. *Front Environ. Sci.* **2022**, *10* (July), 1−12.
(88) Cade-Menun, B. J.; Paytan, A. Nutrient Temperature and Light Stress Alter Phosphorus and Carbon Forms in Culture-Grown Algae. *Mar Chem.* **2010**, *121* (1−4), 27−36.
(89) Voronkov, A.; Sinetova, M. Polyphosphate Accumulation Dynamics in a Population of Synechocystis Sp. PCC 6803 Cells under Phosphate Overplus. *Protoplasma* **2019**, *256* (4), 1153−1164.
(90) Akiyama, M.; Crooke, E.; Kornberg, A. An Exopolyphosphatase of Escherichia Coli. The Enzyme and Its Ppx Gene in a Polyphosphate Operon. *J. Biol. Chem.* **1993**, *268* (1), 633−639.
(91) Lean, D. R. S.; Pick, F. R. Photosynthetic Response of Lake Plankton to Nutrient Enrichment: A Test for Nutrient Limitation. *Limnol Oceanogr* **1981**, *26* (6), 1001−1019.
(92) Borchardt, M. A.; Hoffmann, J. P.; Cook, P. W. Phosphorus Uptake Kinetics of Spirogyra Fluviatilis (Charophyceae) in Flowing Water. *J. Phycol* **1994**, *30*, 403−417.
(93) Battin, T. J.; Besemer, K.; Bengtsson, M. M.; Romani, A. M.; Packmann, A. I. The Ecology and Biogeochemistry of Stream Biofilms. *Nat. Rev. Microbiol* **2016**, *14* (4), 251−263.
(94) Bieroza, M. Z.; Heathwaite, A. L. Seasonal Variation in Phosphorus Concentration-Discharge Hysteresis Inferred from High-Frequency in Situ Monitoring. *J. Hydrol (Amst)* **2015**, *524*, 333.
(95) Lloyd, C. E. M.; Freer, J. E.; Johnes, P. J.; Collins, A. L. Using Hysteresis Analysis of High-Resolution Water Quality Monitoring Data, Including Uncertainty, to Infer Controls on Nutrient and Sediment Transfer in Catchments. *Science of The Total Environment* **2016**, *543*, 388−404.
(96) Evans, D. J.; Johnes, P. J. Physico-Chemical Controls on Phosphorus Cycling in Two Lowland Streams. Part 1 − the Water Column. *Sci. Total Environ.* **2004**, *329*, 145−163.
(97) Biagi, K. M.; Ross, C. A.; Oswald, C. J.; Sorichetti, R. J.; Thomas, J. L.; Wellen, C. C. Novel Predictors Related to Hysteresis and Baseflow Improve Predictions of Watershed Nutrient Loads: An Example from Ontario's Lower Great Lakes Basin. *Sci. Total Environ.* **2022**, *826*, 154023.
(98) Macrae, M. L.; English, M. C.; Schiff, S. L.; Stone, M. Capturing Temporal Variability for Estimates of Annual Hydrochemical Export from a First-Order Agricultural Catchment in Southern Ontario, Canada. *Hydrol Process* **2007**, *21* (13), 1651−1663.

https://doi.org/10.1021/acs.est.2c06285
Environ. Sci. Technol. 2023, 57, 4643−4655